HHS Public Access

Author manuscript

J Invest Dermatol. Author manuscript; available in PMC 2016 April 01.

Published in final edited form as:

J Invest Dermatol. 2015 October ; 135(10): 2464–2474. doi:10.1038/jid.2015.200.

The *CASC15* long intergenic non-coding RNA locus is involved in melanoma progression and phenotype-switching

Laurent Lessard[1], **Michelle Liu**[1], **Diego M. Marzese**[1], **Hongwei Wang**[2], **Kelly Chong**[1], **Neal Kawas**[1], **Nicholas C Donovan**[1], **Eiji Kiyohara**[1], **Sandy Hsu**[1], **Nellie Nelson**[1], **Sivan Izraely**[3], **Orit Sagi-Assif**[3], **Isaac P Witz**[3], **Xiao-Jun Ma**[2], **Yuling Luo**[2], and **Dave SB Hoon**[1]

[1]Department of Molecular Oncology, John Wayne Cancer Institute at Providence St-John's Health Center, 2200 Santa Monica Blvd, Santa Monica, CA, 90404.

[2]Advanced Cell Diagnostics, Inc., 3960 Point Eden Way, Hayward, CA, 94545.

[3]Department of Cell Research and Immunology, The George S. Wise Faculty of Life Sciences, Tel Aviv University, Tel Aviv, 69978, Israel.

Abstract

In recent years, considerable advances have been made in the characterization of protein-coding alterations involved in the pathogenesis of melanoma. However, despite their growing implication in cancer, little is known about the role of long non-coding RNAs in melanoma progression. We *hypothesized* that copy number alterations of intergenic non-protein coding domains could help identify long intergenic non-coding RNAs (lincRNAs) associated with metastatic cutaneous melanoma. Among several candidates, our approach uncovered the chromosome 6p22.3 *CASC15* lincRNA locus as a frequently gained genomic segment in metastatic melanoma tumors and cell lines. The locus was actively transcribed in metastatic melanoma cells, and up-regulation of *CASC15* expression was associated with metastatic progression to brain metastasis in a mouse xenograft model. In clinical specimens, *CASC15* levels increased during melanoma progression and were independent predictors of disease recurrence in a cohort of 141 patients with AJCC stage III lymph node metastasis. Moreover, siRNA knockdown experiments revealed that *CASC15* regulates melanoma cell phenotype switching between proliferative and invasive states. Accordingly, *CASC15* levels correlated with known gene signatures corresponding to melanoma proliferative and invasive phenotypes. These findings support a key role for *CASC15* in metastatic melanoma.

To whom correspondence should be addressed: Dr. Dave S.B. Hoon, Department of Molecular Oncology, John Wayne Cancer Institute at Providence St-John's Health Center, 2200 Santa Monica Blvd, Santa Monica, CA, 90404, hoond@jwci.org.

Data Access

Copy number and exon array gene expression data have been deposited in Gene Expression Omnibus (GEO) under the accession numbers GSE44019 and GSE44660, respectively.

Conflict of Interest

The authors state no conflict of interest.

Supplemental Material

Supplementary material is linked to the online version of the paper at http://www.nature.com/jid

Introduction

In 2014, the rising incidence of cutaneous melanoma continues to outpace most other cancers in the USA (Siegel *et al.*, 2014). The situation is alarming given the high propensity of melanoma lesions to metastasize to many major organ sites, which include liver, lung, and brain. This translates into a 5-year overall survival (OS) rate of less than 20% in patients with AJCC stage IV disease (McDermott *et al.*, 2014). In recent years, the successful development of new FDA approved targeting agents such as vemurafenib/dabrafenib (BRAFmt inhibitors), trametinib (MEK inhibitor), ipilimumab (CTLA-4 antibody) and more recently pembrolizumab (PD-1 antibody) has significantly improved patient survival, but unfortunately most tumors eventually become drug-resistant and undergo lethal progression <2 years after the start of treatment (Alcala and Flaherty, 2012; Ascierto *et al.*, 2013; Hodi *et al.*, 2010; McArthur *et al.*, 2014; Postow *et al.*, 2015). To overcome this issue and expand the number of patients that could benefit from targeted therapies, current research focuses on the identification of melanoma molecular subtypes that could be targeted by specific inhibitor combinations and/or be used as biomarkers to guide treatment decisions (Vidwans *et al.*, 2011). Thus far, considerable progress has been made in the characterization of genetic and epigenetic alterations affecting protein-coding genes and corresponding signaling pathways (Shtivelman *et al.*, 2014). In contrast, aside from miRNAs, less is known about the contribution of non-protein coding genes to melanoma progression. Recently, long noncoding RNAs (lncRNAs) have emerged as important regulators of multiple biological functions in various diseases including cancer (Kung *et al.*, 2013).

Traditionally considered, for the most part, as transcriptional noise resulting from genome-wide pervasive transcription, lncRNAs are now increasingly recognized as master regulators of crucial cellular processes such as cell cycle regulation(Hung *et al.*, 2011), cell-fate and differentiation (Flynn and Chang, 2014), p53 response (Huarte *et al.*, 2010; Marin-Bejar *et al.*, 2013), and chromatin remodeling (Rinn and Chang, 2012). The number of identified long non-coding RNAs is constantly rising: for instance, since 2009, the number of GENCODE annotated long non-coding RNA transcripts has more than doubled, going from ~10,000 to >26,000 in the most recent versions (gencodegenes.org/stats.html). LncRNAs are classified in different sub-groups according to their function or their location based on their intersection with protein-coding genes (Derrien *et al.*, 2012). The latter includes antisense transcripts that share exon(s) with coding genes, sense or antisense transcripts that overlap protein-coding exons, intronic sense/antisense transcripts, and long intergenic (or intervening) non-coding RNAs (lincRNAs) that are located between protein-coding genes. LincRNAs represent the majority of all lncRNAs (Cabili *et al.*, 2011) and although a growing number are now implicated in cancer (Gutschner and Diederichs, 2012), only a few have been characterized in melanoma.

In the present study, driven by the *hypothesis* that recurrent DNA copy number alterations (CNAs) in metastatic melanoma specimens may help identify clinically relevant lincRNAs, we assessed the copy number status of >2300 previously published intergenic domains that were used to uncover actively transcribed lincRNAs in non-melanoma cell lines (Khalil *et al.*, 2009). Our approach identified the *CASC15* locus as a frequently altered lincRNA domain in metastatic melanoma whose transcript levels correlate with disease progression

and function as regulators of metastatic melanoma cell transition between proliferative and invasive states.

Results

Identification of lincRNA domains associated with metastatic melanoma

To uncover lincRNAs involved in metastatic melanoma progression, we assessed the copy number status of 2367 intergenic domains in 78 metastatic melanoma samples (42 cell lines and 36 tissues; see Table S1 for details). These genomic segments were previously identified in non-melanoma cell lines as putative non-protein coding transcriptional units due to the presence of a histone H3 lysine 4 and H3 lysine 36 trimethylation (K4–K36) signature indicative of active transcription (Khalil *et al.*, 2009). We found several CNAs associated with these domains in both melanoma cell lines and tissues (Figure 1a, Tables S2–S3). Most gains and losses were located on chromosome arms frequently altered in metastatic melanoma[1]. However, the alteration pattern of chromosome 6 domains was particularly striking: among the most frequently gained or deleted segments, 34% were located on the 6p arm and 35% on the 6q arm, respectively (Figure 1b; Tables S2–S3). To identify tumor-promoting lincRNAs, we focused downstream analyses on the most frequently gained 6p domains. We identified 18 gained regions with annotated lincRNAs transcripts, 4 of which overlapping between RefSeq and GENCODE v17 databases (Table S4). We then interrogated the TCGA melanoma database (n=278) for CNAs and RNA expression using the cBioPortal (Gao *et al.*, 2013). We confirmed that 2 of these 4 domains, i.e. *CASC15* and *LOC100132354*, were transcribed in melanoma specimens. Most importantly, unlike *LOC100132354*, the frequent copy number gains at the *CASC15* locus were correlated with an increment in *CASC15* expression (Figure S1). Intrigued by this correlation (Spearman's rho: 0.442), we wondered if this could be accompanied by focal amplification of the locus. A closer look at the 6p22.3 region, however, confirmed that *CASC15* gains are associated with arm-level CNAs rather than focal amplifications (Figure 1c and Figure S2). Nevertheless, while *CASC15* remains barely detectable in normal human tissues (Figure S3a), TCGA pan-cancer analysis revealed that melanoma ranks third among 23 tumor types for the highest median *CASC15* expression levels (Figure S3b). Altogether, these findings prompted us to investigate the role of the *CASC15* locus in melanoma.

CASC15 RNA is expressed in melanoma lines and up-regulated in a xenograft model of melanoma brain metastasis

The *CASC15* intergenic locus (NCBI Gene ID: 401237), formerly known as the *LINC00340 or FLJ22536* locus, spans ~530 kilobases (kb) between the *SOX4* and *PRL* genes on chromosome 6p22.3 (Figure 2a; Figure S4). According to the RefSeq database (release 59), the region encodes a predicted poly-adenylated 1900 nucleotide (nt) 12-exon *CASC15* transcript on the plus strand, as well as a poly-adenylated 2300 nt 3-exon *CASC14* transcript on the minus strand, between exons 9 and 10 of *CASC15*. The GENCODE v17 database also includes both lincRNA genes, but *CASC15* is annotated as a 327 basepairs (bp) transcript

[1]Broad Institute TCGA Genome Data Analysis Center (2014): Analysis Overview for Skin Cutaneous Melanoma (Metastatic cohort) - 15 July 2014. Broad Institute of MIT and Harvard. doi:10.7908/C18P5Z9Z

composed of 2 exons that correspond to exons 8 and 9 of the RefSeq annotation. Despite this discrepancy, the existence of multiple spliced Expressed Sequence Tags (ESTs) aligning with the plus strand of the *CASC15* locus indicates that multiple isoforms may be expressed (Figure S4).

We first assessed the expression of *CASC14* and *CASC15* transcripts in cultured melanocytes (primary culture and pMEL-NRAS cell line) and metastatic melanoma cell lines by RT-qPCR using primer pairs targeting *CASC14* exon 3 and *CASC15* exon 8 (conserved between RefSeq, GENCODE v17, and several ESTs; Figure S4). *CASC14* was expressed in all 30 melanoma metastasis cell lines and in pMEL-NRAS cells, but was undetected in cultured melanocytes (Figure S5a). *CASC15* was detected in both melanocyte cultures and 28 of 30 metastatic melanoma lines (Figure 2b). Levels of both lincRNAs were highly variable among cell lines, but were not related to the *BRAF* mutation status of melanoma cells (Figure 2c; Figure S5b).

We then examined *CASC14* and *CASC15* expression levels in a human melanoma xenograft mouse model of brain metastasis (Izraely *et al.*, 2012). In this model, the brain metastasis variant cell line YDFR.SB3 was obtained from the cutaneous variant YDFR.C. Remarkably, *CASC14 and CASC15* transcripts were significantly up-regulated 2- and 17-fold in brain metastasis YDFR.SB3 cells compared to cutaneous YDFR.C cells, and this up-regulation was accompanied by a single copy gain of the *CASC15* locus in YDFR.SB3 cells (Figure 2d). These observations suggest that lincRNAs transcribed from the *CASC15* locus may be associated with melanoma metastasis progression.

RACE identifies an alternative *CASC15* transcriptional start site and multiple splice variants

Given the high number of spliced ESTs associated with the plus strand of the *CASC15* locus (Figure S4), and the significant induction of *CASC15* RNA in the brain metastatic variant YDFR.SB3 (Figure 2d), we performed 5’- and 3’-RACE to determine whether several *CASC15* splice variants were present in melanoma cell lines. Using *CASC15* exon 8 as the template for nested gene-specific primers, we screened cDNA from three metastatic melanoma cell lines and confirmed the existence of several *CASC15* isoforms (Figure 3a; Table S5). Interestingly, we also identified an alternative transcriptional start site (TSS) located between exons 4 and 5 of the predicted RefSeq sequence (exon 1b; Figure 3a; Table S5). These first exon variants aligned with known EST- and CaptureSeq-derived sequences (Figure S4; (Mercer *et al.*, 2012)). We assessed the protein coding potential of the cloned isoforms using the CPAT algorithm (Wang *et al.*, 2013), and found that all sequences had low coding capacity similar to the annotated sequences (Table S5). In addition, scanning the putative full-length *CASC15* isoforms sequences against the Pfam database (Finn *et al.*, 2014) did not retrieve any catalogued protein family domains.

We then assessed the expression levels of different groups of isoforms by RT-qPCR, and observed strong positive correlations between each cloned variants (Figure S6). On average, absolute quantification revealed that isoforms downstream of the alternative TSS were expressed at 0.35 copies per cell (or 15ng of total RNA; Figure 3b). In contrast, RefSeq-annotated exons 1–2 and 4–5 located upstream of the alternative TSS were barely detectable

(<0.01 copy). This finding supports 5'-RACE cloning results and suggests an important role of the alternative TSS in melanoma cells. We also analyzed the subcellular localization (cytoplasm vs. nucleus) of the cloned splice variants and although they could be detected in both compartments, we observed a tendency towards nuclear enrichment similar to the well-characterized HOTAIR lincRNA (Figure 3c). In summary, these findings confirm that metastatic melanoma cells express several *CASC15* splice variants originating from an alternative TSS and predominantly localized in the cell nucleus. These data were also useful for the accurate detection and silencing of *CASC15* transcripts in clinicopathological and functional analyses.

CASC15 levels increase during melanoma progression

We next examined tissue expression levels of *CASC15* transcripts. Using RT-qPCR, we assessed the levels of both exon 8- and exons 10–11-containing isoforms in 70 formalin-fixed paraffin-embedded (FFPE) tissue samples. As for metastatic melanoma cell lines, we found a positive correlation between the levels of both isoform groups (Figure S7a). With regards to melanoma progression, *CASC15* expression was significantly increased in advanced stage IV melanomas (brain and lung metastases) relative to normal skin and nevus specimens (T-test; $P<0.01$; Figure 4e; Figure S7b).

To better characterize *in situ* expression levels and subcellular distribution of *CASC15* transcripts, we performed RNA *in situ* hybridization (RNA-ISH) on 62 FFPE specimens using RNAscope technology as shown in Figure 4a–d (Wang *et al*., 2012). The target sequence, covering *CASC15* exons 5 to 12, was designed for optimal sensitivity and to detect a maximum number of expressed isoforms. In general, *CASC15* RNA detection was restricted to melanoma cells and absent from other non-melanoma cell types, except for rare lymphocyte positivity. Most positive cells expressed 1 to 10 *CASC15* copies, but >10 copies were also observed in 1–10% of melanoma cells in different tumors (Figures 4d and 4g). Consistent with our RT-qPCR cell line results (Figure 3c), *CASC15* RNA was principally located in the nucleus of melanoma cells, but also detected in the cytoplasm (Figures 4a–d). Most importantly, we noticed significant differential expression of *CASC15* during melanoma progression (Kruskal-Wallis test, $P<0.01$; Figure 4f). In particular, we observed higher *CASC15* levels in stage III LN metastases relative to non-malignant specimens (Mann-Whitney test; $P<0.01$), as well as increased *CASC15* levels in stage IV brain and lung lesions relative to stage III LN metastases (Mann-Whitney test; $P<0.05$; Figure 4f). Collectively, these findings align with the results of our xenograft mouse model of brain metastasis, and further support a role for *CASC15* in melanoma progression from early stages to stage IV metastasis.

CASC15 expression in melanoma LN metastases is an independent predictor of disease recurrence and survival

We then sought to determine whether *CASC15* expression, which also displayed substantial inter-patient variability (Figures 4e–f), could be used to stratify patients at low- and high-risk of metastatic melanoma progression to stage IV melanoma. We performed RNA-ISH as described above on a TMA containing 141 FFPE LN metastasis specimens. Again, we noticed strong inter-patient variability and a mean frequency of *CASC15*-positive melanoma

cells per LN metastasis (mean: 23%; %CV: 103%) similar to our findings in the first cohort (mean: 18%; %CV: 129%; Figure 4f). Subsequent Kaplan-Meier analysis of disease-free and overall survival (DFS and OS, respectively) showed that patients with elevated *CASC15* expression had significantly shorter DFS compared to low *CASC15*-expressing patients (Figure 4h; Figure S7c). Moreover, in stepwise multivariable Cox regression analyses, *CASC15* expression improved the predictive strength of multivariate models of stage III melanoma outcome (DFS: $P<0.05$; OS: $P<0.01$) over clinical variable-only models (Table S6). Taken together, these findings support the prognostic significance of *CASC15* expression in metastatic melanoma.

CASC15 silencing in melanoma cell lines induces a phenotype switch

To characterize the function of *CASC15* transcripts, we performed RNAi-mediated silencing using siRNA pools targeting most *CASC15* isoforms identified in the RACE experiments. We first assessed *CASC15* knockdown efficiency, and selected three high *CASC15*-expressing cell lines (WP, M16, and RKTJ-CB1) showing consistent reduction in all four isoform groups examined (Figure S8). With the exception of siPool1-transfected RKTJ-BI3 cells, *CASC15* silencing by both siRNA pools had an important inhibitory effect melanoma cell clonogenic growth (Figure 5a), The inhibition was consistently more pronounced in siPool2 conditions (Figure 5a) and always accompanied by a significant increase in melanoma cell invasiveness (Figure 5b), a phenomenon reminiscent of melanoma cell phenotype-switching between proliferative and invasive states. The underlying siPool2-induced alterations in cell cycle kinetics and baseline survival were cell type-specific (Figure S9), and involved a decreased rate in DNA synthesis (M16), a combination of decreased DNA synthesis and increased cell death (RKTJ-BI3), or increased DNA synthesis counterbalanced by increased cell death (WP). The Interestingly, RKTJ-CB1 cells responded differently to siPool1-mediated silencing, showing the reverse pattern: an increased clonogenic growth and a decline in invasive properties (Figure 5a–b). Consistently, this effect was associated with a modest but significant increase in the rate of DNA synthesis (Figure S9a).

To gather additional evidence for a role of CASC15 in phenotype-switching, we performed expression arrays to assess whether variations of *CASC15* levels (exons 5–12) in metastatic melanoma cell lines (n=47) could discriminate between the previously reported proliferative (motif 1) and invasive (motif 2) melanoma gene signatures associated with this process (Hoek *et al.*, 2006; Stanisz *et al.*, 2014). As expected, the 2 signatures were inversely correlated (Figure 5c, Table S7), thus validating published findings (Hoek *et al.*, 2006). Interestingly, we found that *CASC15* expression was both positively correlated with a large subset of proliferative genes, and inversely correlated with several invasion-related genes (Figure 5c, Table S7). Most importantly, RNA sequencing of siPool2-mediated *CASC15* knockdown in all 3 cell lines identified a down-regulation of 31 proliferative signature genes, including the master regulator transcription factors *MITF* and *SOX10*, and a concomitant up-regulation of 21 invasive signature genes (Figure 5d, Table S8). Overall, these results underscore the functional complexity of *CASC15* transcripts, and position *CASC15* transcripts as candidate regulators of melanoma phenotype-switching.

Discussion

In recent years, long non-coding RNAs have emerged as important regulators of cellular homeostasis and cell fate (Flynn and Chang, 2014; Kung *et al.*, 2013), whereby the number of long non-coding RNAs implicated in tumorigenesis and other diseases is growing rapidly (Gutschner and Diederichs, 2012). In melanoma, only a limited number have been identified and functionally investigated (Aftab *et al.*, 2014; Flockhart *et al.*, 2012; Khaitan *et al.*, 2011; Tang *et al.*, 2013; Tian *et al.*, 2014; Wu *et al.*, 2013). For instance, the intronic long non-coding RNA SPRY4-IT1 has been identified as a melanoma up-regulated transcript with anti-apoptotic and pro-invasive functions (Khaitan *et al.*, 2011; Mazar *et al.*, 2014), and the lincRNA BANCR has been characterized as a BRAFmt-regulated transcript involved in melanoma cell migration (Flockhart *et al.*, 2012). In the present study, we sought to expand upon the literature of melanoma-associated lncRNAs by analyzing copy number alterations of non-protein coding intergenic domains in metastatic melanoma. Our screening uncovered a large number of frequently altered putative lincRNA domains. We noticed a particularly high concentration of gained intergenic domains on chromosome 6p, suggesting that this chromosome arm may be a possible hotspot for tumor-promoting lincRNAs that warrants further investigation. While we acknowledge that the number of currently annotated lincRNA genes (or transcriptional units) largely exceeds the number of analyzed intergenic domains, our strategy was nonetheless successful in identifying a clinically and functionally relevant lincRNA locus and justifies the pursuit of more comprehensive genome-wide integrative studies.

The *CASC15* locus was originally identified *in silico* as a highly active, non-protein coding transcriptional unit with several associated ESTs and mRNAs (Glusman *et al.*, 2006). Subsequently, an independent genome-wide association study (GWAS) reported that 3 intronic single nucleotide polymorphisms (SNPs) within the *CASC15* locus (between exons 9 and 10) were strongly associated with clinically aggressive neuroblastoma (Maris *et al.*, 2008). More recently, one of these SNPs has been linked to *CASC14* expression levels (also known as *NBAT-1*) that are shown to play a pivotal role in neuroblastoma progression (Pandey *et al.*, 2014). Our results revealed a similar association with aggressive tumors, linking the *CASC15* locus and related transcripts to metastatic melanoma progression. Whether the high-risk SNPs identified in neuroblastoma are also associated with aggressive melanomas remains to be tested but like other lncRNAs such as *ANRIL* (Burd *et al.*, 2010) and *CCAT2* (Ling *et al.*, 2013), they may affect the splicing and/or expression of *CASC15* transcripts.

RACE analyses confirmed that melanoma lines express a remarkable variety of alternatively spliced *CASC15* isoforms and exon variants. An even greater number may be present in melanoma cells since our RACE experiments only focused on exon 8-containing transcripts that were conserved between RefSeq (release 59) and GENCODE v17 annotations, as well as several ESTs. This splice variant complexity has been observed for other well-characterized lncRNAs such as *ANRIL* (Burd *et al.*, 2010), *MEG3* (Zhang *et al.*, 2010), and *CRNDE* (Ellis *et al.*, 2012), and proposed to confer variant-specific structural properties affecting their function. With regards to *CASC15* isoforms, alternative splicing may dictate their subcellular distribution: despite overall nuclear enrichment of *CASC15* transcripts, the

nuclear/cytoplasmic ratio of exon 8-containing isoforms was consistently higher than exons 10–11- and 11–12-containing isoforms, a pattern that may reflect variable functions. Some of the linear isoforms detected in our RACE experiments could also be by-products of circular RNA (circRNA) genesis, a likely possibility given the reported existence of a highly-expressed 204 nt circRNA isoform emanating from the *CASC15* locus (Salzman *et al.*, 2013). In addition to splice variants, we found that melanoma cells preferentially express transcripts from an alternative TSS, which may also be important for *CASC15* isoform function. Dissecting out the roles of individual *CASC15* isoforms will be a challenging task, but the locus nonetheless represents an exquisite model to study the transcriptional regulatory mechanisms controlling lncRNA biogenesis.

While *CASC15* isoforms may exert specific functions, our findings demonstrate that their global up-regulation is associated with melanoma progression to advance stages of distant metastasis. Moreover, *CASC15* levels can be used to discriminate between patients at low- and high-risk of disease progression. The ability of *CASC15* expression levels to predict AJCC stage III melanoma recurrence is important given the pressing need for biomarkers predictive of melanoma progression to stage IV disease (Eggermont *et al.*, 2014). To fully exploit the potential of novel targeted therapies, stage IV melanoma needs to be diagnosed earlier for prompt treatment, ideally before evidence of widespread dissemination. In this context, *CASC15* merits further independent validation to confirm its prognostic utility in melanoma patients.

To our knowledge, *CASC15* knockdown experiments uncovered previously unreported role for lncRNAs in the regulation of melanoma cell transition between proliferative and invasive states. Inherent to phenotype-switching is the stem cell-like plasticity of melanoma cells (Hoek and Goding, 2010), a property in line with the well-recognized involvement of lncRNAs in the regulation of pluripotency and differentiation (Flynn and Chang, 2014; Hu *et al.*, 2012). LncRNAs have been shown to be critical for embryonic stem cell maintenance/differentiation (e.g.: *RNCR2*, *Xist*), induced pluripotent stem cell reprogramming (e.g.: *linc-ROR*), neural progenitor differentiation (e.g.: *lncRNA_N1–3*; RMST), and adult somatic progenitor cell maintenance (e.g.: *ANCR*). The regulation of phenotype-switching by *CASC15* adds to these lncRNA-mediated stem cell-like functions, and provides the grounds for future studies addressing the contribution of *CASC15* transcripts to melanoma initiating/stem cell maintenance. In particular, it would be interesting to assess whether *CASC15* transcripts directly regulate the master melanoma oncogene *MITF* and/or its upstream inducer *SOX10*, given their known implication in melanocyte stem cell fate and phenothype-switching (Hoek and Goding, 2010), and their down-regulation upon *CASC15* knockdown (Figure 5d, Table S8).

The silencing of *CASC15* transcripts had a drastic impact on melanoma cell phenotype. Moreover, especially in RKTJ-CB1 cells, our findings suggest that *CASC15*-targeting siRNAs can exert opposite effects despite similar knockdown efficiencies (Figure S8). Although some isoforms not covered by our RT-qPCR assays could be differentially silenced, another likely explanation could reside in the sequences targeted by the two siRNA pools, some of which may be critical for *CASC15* function(s). For instance, specific

sequences may interact with RNA/DNA or proteins, and/or may encode small functional peptides involved in the regulation of proliferative or invasive states (Bazzini *et al.*, 2014).

In summary, analysis of altered intergenic domains in metastatic melanoma uncovered the *CASC15* locus as a frequently gained region with tumor-promoting properties. *CASC15* lincRNA isoforms are associated with melanoma progression and disease recurrence, and play a key role in melanoma phenotype-switching. Our study represents a largely unexplored area of melanoma molecular biology, and support the functional relevance of lincRNAs in melanoma progression.

Materials and Methods

Melanoma specimens and cell lines

Frozen and FFPE tissues were obtained under an institutional review board (IRB) protocol that was approved by the Saint John's Health Center (SJHC)/John Wayne Cancer Institute (JWCI) joint IRB and Western IRB. Written informed consent was obtained for all subjects. Melanoma cell lines and immortalized pMEL-NRAS(G12D) melanocytes (gift from Dr. Levi Garraway, Broad Institute, Cambridge, MA), were cultured in RPMI-1640 medium as already described (Marzese *et al.*, 2014a). Primary human melanocytes (Life Technologies, Carlsbad, CA) were cultured in Medium 254 supplemented with human melanocyte growth supplement-2, PMA-Free (HMGS-2). See Supplementary Materials and Methods for more details.

Nucleic acid extraction and BRAF sequencing

DNA from frozen tissues and cell lines was extracted using the QiAmp DNA mini kit (Qiagen, Valencia, CA), and quantified with the Quant-iT PicoGreen double-stranded DNA Kit (Life Technologies). Direct sequencing (Eurofins, Hunstville, AL) was used for the assessment of BRAF mutational status as previously reported (Marzese *et al.*, 2014b). Total RNA was extracted from cell lines using TriReagent (Molecular Research Center, Inc., Cincinnati, OH) and from FFPE tissues using RNA-Solv Reagent (Omega Bio-Tek, Norcross, GA) according to the manufacturers' instructions. Isolation of nuclear and cytoplasmic RNA was performed using the PARIS Kit (Life Technologies). RNA concentration was quantified and qualified by UV absorption spectrophotometry and the Quant-iT RiboGreen RNA Assay Kit (Life Technologies).

DNA copy number profiling

Genotyping of DNA from melanoma specimens (n=78, Table S1) was performed using the Affymetrix Genome-Wide SNP 6.0 array and analyzed using Genotyping Console 4.0 (Affymetrix) as previously described (Marzese *et al.*, 2014a). More details are provided in the Supplementary Materials and Methods section.

Reverse transcription and quantitative real-time PCR (RT-qPCR)

Reverse-transcription (RT) of total RNA was performed as previously described (Marzese *et al.*, 2014a). Prior to RT, we performed DNase treatment on all the samples using the TURBO DNA-free Kit according to the manufacturer's instructions (Life Technologies).

The CFX96 Real-Time PCR Detection System (Bio-Rad Laboratories, Hercules, CA) was used for qPCR amplification. Refer to Supplementary Materials and Methods for more details.

Rapid amplification of cDNA ends (RACE)

The FirstChoice RLM-RACE Kit (Life Technologies) was used for 5'- and 3'-RACE identification of *CASC15* isoforms. *CASC15* exon8-specific outer and inner primers are listed in Table S9. See Supplementary Materials and Methods for more details.

RNA in situ hybridization (RNA-ISH)

The RNAscope RNA-ISH protocol was performed as previously described (Wang *et al.*, 2012). RNA quality control (human *ubiquitin C* gene) and negative control (bacterial *dapB* gene) probes were used on each FFPE specimen. Scoring was performed by two independent investigators (L.L. and H.W.) who examined whole tumor sections (or TMA cores) for *CASC15* staining. The RNAscope Fluorescent Assay was also used as previously described (Wang *et al.*, 2012) on M16 and WP cell lines to assess the specificity of *CASC15* probes (Figure S10).

Clonogenic growth and invasion assays

For clonogenic assays, cells were plated in 6-well plates 24h following siRNA transfection at a density of 5000 (WP), 2000 (M16), and 1000 (RKTJ-CB1) cells per well. Medium was refreshed the next day, and changed every 3 days until colonies reached a size of ~50 cells (10–13 days after plating). Colonies were then fixed in 0.5% crystal violet in methanol. Images of each well were captured using MyECL imager (Thermo Scientific, Waltham, MA) and colony number was quantified using the Image J software (Bethesda, MD) with a particle size threshold of ≥4 pixels for colonies ≥ 50-cells. Melanoma cell invasion was assessed using a transwell matrigel chamber system following the manufacturer's instructions (BD Biosciences, San Diego, CA). See Supplementary Materials and Methods for more details.

Genome-wide gene expression profiling

Genome-wide exon array gene expression profiling in melanoma cell lines (n=47, Table S1, Figure 5c) was performed as already described (Marzese *et al.*, 2014a). For *CASC15*, probes targeting exons 5 to 12 (RefSeq annotation) were used to determine overall *CASC15* expression levels. For total RNA sequencing (Figure 5d), details are provided in the Supplementary Materials and Methods section.

Statistics

Statistical analyses were performed using the Prism 5.0 GraphPad Software (La Jolla, CA) and the JMP 8 statistical package (SAS Institute, Inc., Cary, NC). A detailed description of all statistical tests is provided in the Supplementary Materials and Methods section.

Supplementary Material

Refer to Web version on PubMed Central for supplementary material.

Acknowledgments

This work was supported by the Dr. Miriam and Sheldon G. Adelson Medical Research Foundation, the Ruth and Martin H. Weil Fund, as well as the award numbers PO1 CA029605 (Project II and Core C) and 1R01CA167967-01A1 from the National Cancer Institute, National Institutes of Health. We are also grateful to members of the Department of Molecular Oncology at JWCI for their technical assistance and helpful discussions.

Abbreviations

CASC15	cancer susceptibility candidate 15
CNA	copy number alteration
DFS	disease-free survival
EST	expressed sequence tag
FFPE	formalin-fixed paraffin-embedded
lincRNA	long intergenic non-coding RNA
LN	lymph node
OS	overall survival
RACE	rapid amplification of cDNA ends
RNA-ISH	RNA in situ hybridization
RT-qPCR	reverse transcription and quantitative PCR
TMA	tissue microarray
TSS	transcriptional start site

References

Aftab MN, Dinger ME, Perera RJ. The role of microRNAs and long non-coding RNAs in the pathology, diagnosis, and management of melanoma. Arch Biochem Biophys. 2014; 563C:60–70. [PubMed: 25065585]

Alcala AM, Flaherty KT. BRAF inhibitors for the treatment of metastatic melanoma: clinical trials and mechanisms of resistance. Clin Cancer Res. 2012; 18:33–39. [PubMed: 22215904]

Ascierto PA, Minor D, Ribas A, et al. Phase II trial (BREAK-2) of the BRAF inhibitor dabrafenib (GSK2118436) in patients with metastatic melanoma. J Clin Oncol. 2013; 31:3205–3211. [PubMed: 23918947]

Bazzini AA, Johnstone TG, Christiano R, et al. Identification of small ORFs in vertebrates using ribosome footprinting and evolutionary conservation. EMBO J. 2014; 33:981–993. [PubMed: 24705786]

Burd CE, Jeck WR, Liu Y, et al. Expression of linear and novel circular forms of an INK4/ARF-associated non-coding RNA correlates with atherosclerosis risk. PLoS Genet. 2010; 6:e1001233. [PubMed: 21151960]

Cabili MN, Trapnell C, Goff L, et al. Integrative annotation of human large intergenic noncoding RNAs reveals global properties and specific subclasses. Genes Dev. 2011; 25:1915–1927. [PubMed: 21890647]

Derrien T, Johnson R, Bussotti G, et al. The GENCODE v7 catalog of human long noncoding RNAs: analysis of their gene structure, evolution, and expression. Genome Res. 2012; 22:1775–1789. [PubMed: 22955988]

Eggermont AM, Spatz A, Robert C. Cutaneous melanoma. Lancet. 2014; 383:816–827. [PubMed: 24054424]

Ellis BC, Molloy PL, Graham LD. CRNDE: A Long Non-Coding RNA Involved in CanceR, Neurobiology, and DEvelopment. Front Genet. 2012; 3:270. [PubMed: 23226159]

Finn RD, Bateman A, Clements J, et al. Pfam: the protein families database. Nucleic Acids Res. 2014; 42:D222–D230. [PubMed: 24288371]

Flockhart RJ, Webster DE, Qu K, et al. BRAFV600E remodels the melanocyte transcriptome and induces BANCR to regulate melanoma cell migration. Genome Res. 2012; 22:1006–1014. [PubMed: 22581800]

Flynn RA, Chang HY. Long Noncoding RNAs in Cell-Fate Programming and Reprogramming. Cell Stem Cell. 2014; 14:752–761. [PubMed: 24905165]

Gao J, Aksoy BA, Dogrusoz U, et al. Integrative analysis of complex cancer genomics and clinical profiles using the cBioPortal. Sci Signal. 2013; 6:pl1. [PubMed: 23550210]

Glusman G, Qin S, El-Gewely MR, et al. A third approach to gene prediction suggests thousands of additional human transcribed regions. PLoS Comput Biol. 2006; 2:e18. [PubMed: 16543943]

Gutschner T, Diederichs S. The hallmarks of cancer: a long non-coding RNA point of view. RNA Biol. 2012; 9:703–719. [PubMed: 22664915]

Hodi FS, O'Day SJ, McDermott DF, et al. Improved survival with ipilimumab in patients with metastatic melanoma. N Engl J Med. 2010; 363:711–723. [PubMed: 20525992]

Hoek KS, Goding CR. Cancer stem cells versus phenotype-switching in melanoma. Pigment Cell Melanoma Res. 2010; 23:746–759. [PubMed: 20726948]

Hoek KS, Schlegel NC, Brafford P, et al. Metastatic potential of melanomas defined by specific gene expression profiles with no BRAF signature. Pigment Cell Res. 2006; 19:290–302. [PubMed: 16827748]

Hu W, Alvarez-Dominguez JR, Lodish HF. Regulation of mammalian cell differentiation by long non-coding RNAs. EMBO Rep. 2012; 13:971–983. [PubMed: 23070366]

Huarte M, Guttman M, Feldser D, et al. A large intergenic noncoding RNA induced by p53 mediates global gene repression in the p53 response. Cell. 2010; 142:409–419. [PubMed: 20673990]

Hung T, Wang Y, Lin MF, et al. Extensive and coordinated transcription of noncoding RNAs within cell-cycle promoters. Nat Genet. 2011; 43:621–629. [PubMed: 21642992]

Izraely S, Sagi-Assif O, Klein A, et al. The metastatic microenvironment: brain-residing melanoma metastasis and dormant micrometastasis. Int J Cancer. 2012; 131:1071–1082. [PubMed: 22025079]

Khaitan D, Dinger ME, Mazar J, et al. The melanoma-upregulated long noncoding RNA SPRY4-IT1 modulates apoptosis and invasion. Cancer Res. 2011; 71:3852–3862. [PubMed: 21558391]

Khalil AM, Guttman M, Huarte M, et al. Many human large intergenic noncoding RNAs associate with chromatin-modifying complexes and affect gene expression. Proc Natl Acad Sci U S A. 2009; 106:11667–11672. [PubMed: 19571010]

Kung JT, Colognori D, Lee JT. Long noncoding RNAs: past, present, and future. Genetics. 2013; 193:651–669. [PubMed: 23463798]

Ling H, Spizzo R, Atlasi Y, et al. CCAT2, a novel noncoding RNA mapping to 8q24, underlies metastatic progression and chromosomal instability in colon cancer. Genome Res. 2013; 23:1446–1461. [PubMed: 23796952]

Marin-Bejar O, Marchese FP, Athie A, et al. Pint lincRNA connects the p53 pathway with epigenetic silencing by the Polycomb repressive complex 2. Genome Biol. 2013; 14:R104. [PubMed: 24070194]

Maris JM, Mosse YP, Bradfield JP, et al. Chromosome 6p22 locus associated with clinically aggressive neuroblastoma. N Engl J Med. 2008; 358:2585–2593. [PubMed: 18463370]

Marzese DM, Scolyer RA, Huynh JL, et al. Epigenome-wide DNA methylation landscape of melanoma progression to brain metastasis reveals aberrations on homeobox D cluster associated with prognosis. Hum Mol Genet. 2014a; 23:226–238. [PubMed: 24014427]

Marzese DM, Scolyer RA, Roque M, et al. DNA methylation and gene deletion analysis of brain metastases in melanoma patients identifies mutually exclusive molecular alterations. Neuro Oncol. 2014b; 16:1499–1509. [PubMed: 24968695]

Mazar J, Zhao W, Khalil AM, et al. The functional characterization of long noncoding RNA SPRY4-IT1 in human melanoma cells. Oncotarget. 2014; 5:8959–8969. [PubMed: 25344859]

McArthur GA, Chapman PB, Robert C, et al. Safety and efficacy of vemurafenib in BRAF(V600E) and BRAF(V600K) mutation-positive melanoma (BRIM-3): extended follow-up of a phase 3, randomised, open-label study. Lancet Oncol. 2014; 15:323–332. [PubMed: 24508103]

McDermott D, Lebbe C, Hodi FS, et al. Durable benefit and the potential for long-term survival with immunotherapy in advanced melanoma. Cancer Treat Rev. 2014; 40:1056–1064. [PubMed: 25060490]

Mercer TR, Gerhardt DJ, Dinger ME, et al. Targeted RNA sequencing reveals the deep complexity of the human transcriptome. Nat Biotechnol. 2012; 30:99–104. [PubMed: 22081020]

Pandey GK, Mitra S, Subhash S, et al. The Risk-Associated Long Noncoding RNA NBAT-1 Controls Neuroblastoma Progression by Regulating Cell Proliferation and Neuronal Differentiation. Cancer Cell. 2014; 26:722–737. [PubMed: 25517750]

Postow MA, Callahan MK, Wolchok JD. Immune Checkpoint Blockade in Cancer Therapy. J Clin Oncol. 2015 10.1200/JCO.2014.59.4358.

Rinn JL, Chang HY. Genome regulation by long noncoding RNAs. Annu Rev Biochem. 2012; 81:145–166. [PubMed: 22663078]

Salzman J, Chen RE, Olsen MN, et al. Cell-type specific features of circular RNA expression. PLoS Genet. 2013; 9:e1003777. [PubMed: 24039610]

Shtivelman E, Davies MQ, Hwu P, et al. Pathways and therapeutic targets in melanoma. Oncotarget. 2014; 5:1701–1752. [PubMed: 24743024]

Siegel R, Ma J, Zou Z, et al. Cancer statistics, 2014. CA Cancer J Clin. 2014; 64:9–29. [PubMed: 24399786]

Stanisz H, Saul S, Muller CS, et al. Inverse regulation of melanoma growth and migration by Orai1/STIM2-dependent calcium entry. Pigment Cell Melanoma Res. 2014; 27:442–453. [PubMed: 24472175]

Tang L, Zhang W, Su B, et al. Long noncoding RNA HOTAIR is associated with motility, invasion, and metastatic potential of metastatic melanoma. Biomed Res Int. 2013; 2013:251098. [PubMed: 23862139]

Tian Y, Zhang X, Hao Y, et al. Potential roles of abnormally expressed long noncoding RNA UCA1 and Malat-1 in metastasis of melanoma. Melanoma Res. 2014; 24:335–341. [PubMed: 24892958]

Vidwans SJ, Flaherty KT, Fisher DE, et al. A melanoma molecular disease model. PLoS One. 2011; 6:e18257. [PubMed: 21479172]

Wang F, Flanagan J, Su N, et al. RNAscope: a novel in situ RNA analysis platform for formalin-fixed, paraffin-embedded tissues. J Mol Diagn. 2012; 14:22–29. [PubMed: 22166544]

Wang L, Park HJ, Dasari S, et al. CPAT: Coding-Potential Assessment Tool using an alignment-free logistic regression model. Nucleic Acids Res. 2013; 41:e74. [PubMed: 23335781]

Wu CF, Tan GH, Ma CC, et al. The non-coding RNA llme23 drives the malignant property of human melanoma cells. J Genet Genomics. 2013; 40:179–188. [PubMed: 23618401]

Zhang X, Rice K, Wang Y, et al. Maternally expressed gene 3 (MEG3) noncoding ribonucleic acid: isoform structure, expression, and functions. Endocrinology. 2010; 151:939–947. [PubMed: 20032057]

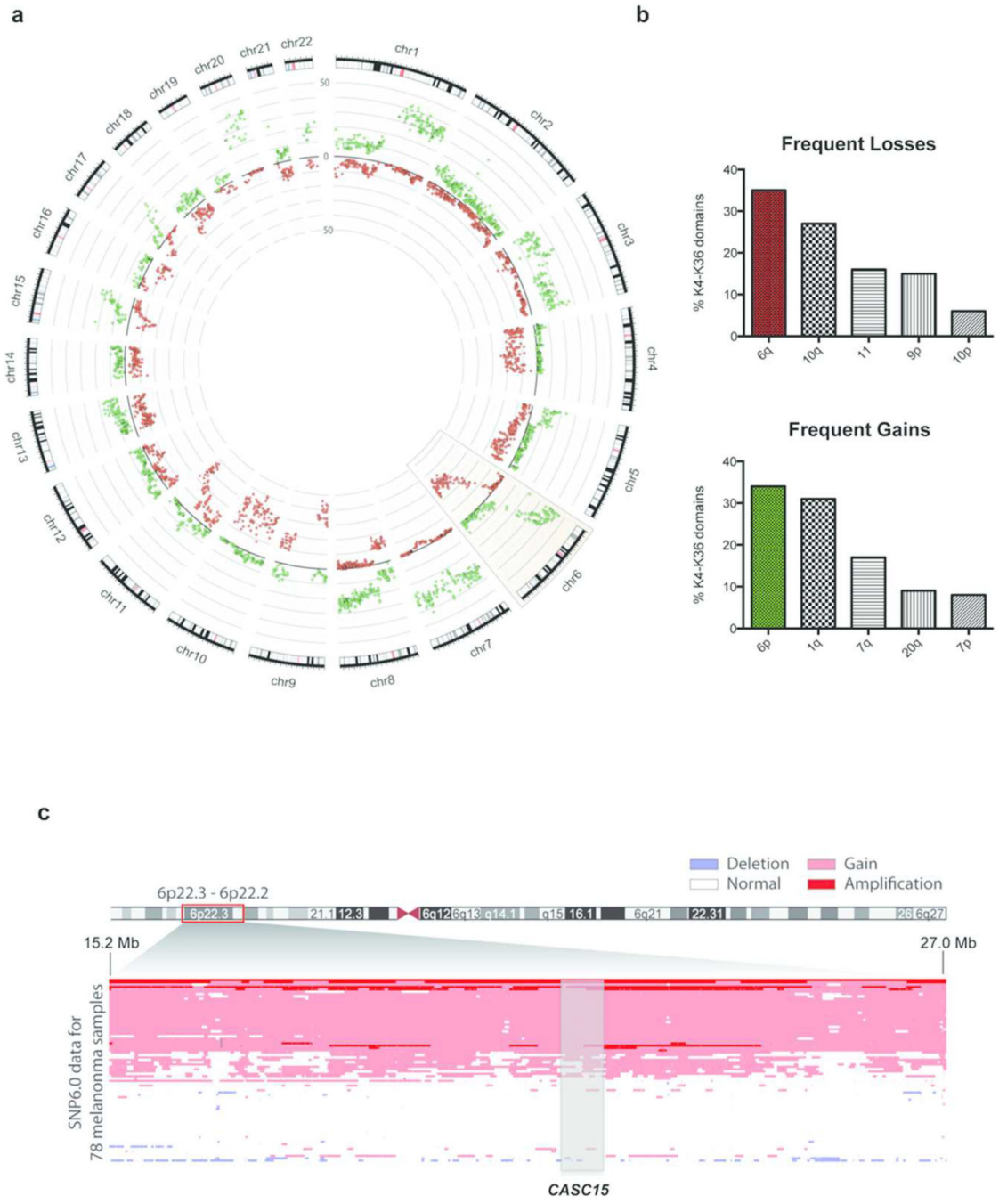

Figure 1.

Copy number alterations of "K4-K36" intergenic domains in metastatic melanoma cell lines and tissues. (**a**) Circos plot depicting copy number alterations (CNAs) of 2367 intergenic domains identified in (Khalil *et al.*, 2009). Each green (or red) dot represents the number of metastatic melanoma specimens that showed copy number gain (or loss) of a specific domain. (**b**) Frequency (%) of the most recurrent CNAs as a function of chromosome arm. Top graph: frequent copy number losses (in >30% of specimens); red bar highlights chromosome 6q alterations. Lower graph: copy number gains (in >40% of specimens); green

bar highlights chromosome 6p alterations. (**c**) Plot-zooming of the chromosome 6p22.3-22.2 region representing copy number data for the 78 melanoma specimens interrogated in (a). Each row represents a patient.

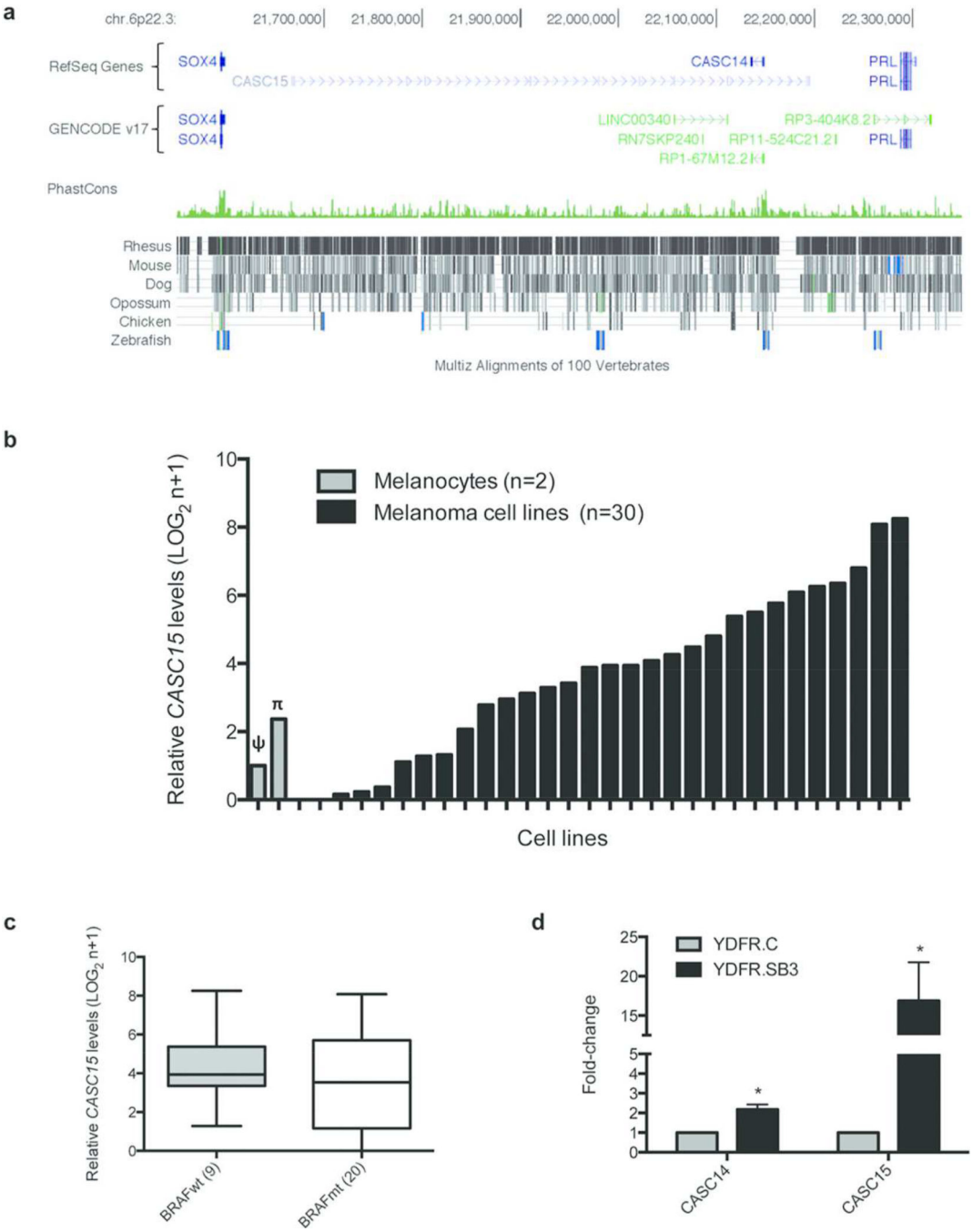

Figure 2.

The 6p22.3 *CASC15* lincRNA locus is actively transcribed in melanoma cell lines. (**a**) UCSC genome browser-derived representation of the *CASC15* locus on chromosome 6p22.3 (GRCh37/hg19 assembly), along with RefSeq and GENCODE v17 annotated genes, PhastCons conservation levels, and Multiz Alignments. (**b**) RT-qPCR detection of *CASC15* (exon 8) levels in melanocytes (grey bars, n=2; ψ: pMEL-NRAS; π: primary melanocytes) and melanoma cell lines (black bars, n=30). (LOG_2 (n+1) of $2^{-(ddCq)}$ relative values) (**c**) *CASC15* expression (RT-qPCR; exon 8) in BRAF wild-type (BRAFwt; *N*=9) and BRAF

mutant (BRAFmt; *N*=20) melanoma cell lines. BRAFmt includes V600E (*N*=16), V600K (*N*=3), and V600R (*N*=1) (LOG_2 (n+1) of $2^{-(ddCq)}$ relative values; Whiskers Min to Max; T-test, *P*>0.05). (**d**) Relative *CASC15* and *CASC14* expression levels (RT-qPCR; exon 8) in a xenograft model of melanoma brain metastasis. Grey bars: Parental YDFR.C cell line. Black Bars: Brain metastasis variant YDFR.SB3 ($2^{-(ddCq)}$ value relative to parental cells, T-test, *, *P*<0.05; Mean +/− SEM, *N*=3).

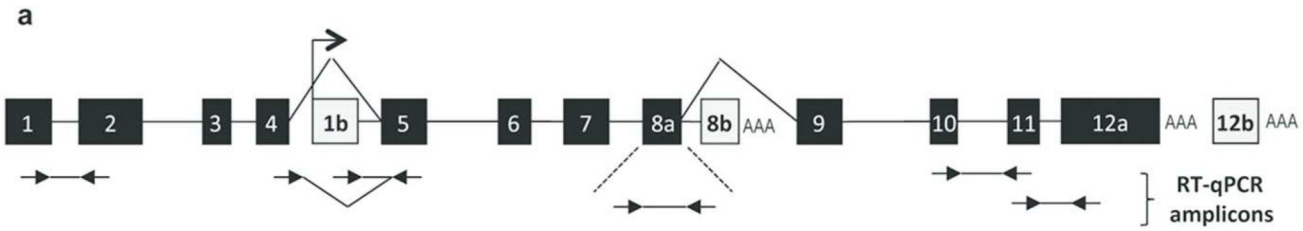

Assay	YDFR.SB3	WP	RKTJ-CB1
5'RACE	***1b***,5,6,7,8a	***1b'***,5,6,8a	***1b''***,5,8a
3'RACE	8a,9.3	8a	8a
	8a,9.2,***12b***	8a,9.4	8a,***8b***
	8a,9.1,11,12a-1	8a,11,12a-4	8a,9.5
	8a,9.2,11,12a-2	8a,***12b***	8a,9.4
	8a,9.2,11,12a-3		8a,9.6
	8a,10,11,12a-2		8a,9.1,***12b***
	8a,10,***12b***		8a,9.1,11,12a-1
	8a,***12b***		8a,9.2,11,12a-4
	8a,11,12a-1		8a,9.2,11,12a-1
	8a,11,12a-3		8a,10,11,12a-2
			8a,11,12a-1
			8a,11,12a-4
			8a,***12b***

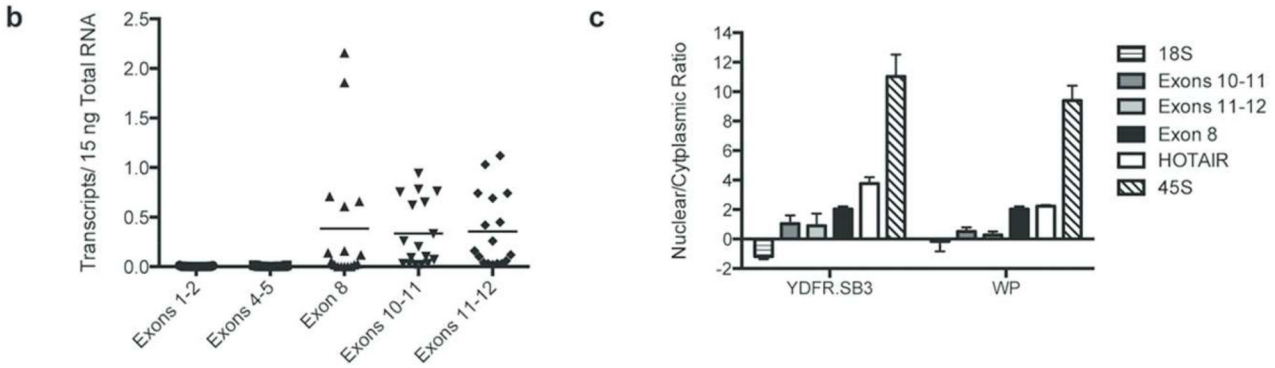

Figure 3.

Melanoma cells express several *CASC15* isoforms transcribed from an alternative transcriptional start site. (**a**) *Top*: Graphical representation of the 12-exon RefSeq-annotated *CASC15* transcript (black exons) as well as additional exons identified by RACE in melanoma cell lines (grey exons labeled 1b (alternative TSS), 8b, and 12b). Regions/exons selected for RT-qPCR are also shown. *Bottom*: 5'- and 3'-RACE variants detected in CSB3, WP, and RKTJ-CB1 metastatic melanoma cell lines. (**b**) Absolute quantification of *CASC15* isoform levels in melanoma cell lines (n=17). Horizontal bars: Mean. (**c**) Nuclear/

Cytoplasmic ratio of *CASC15* isoforms in YDFR.SB3 and WP melanoma cell lines. Values <0 are indicative of cytoplasmic enrichment; values >0 are indicative of nuclear enrichment. (ddCq (Cytoplasm-Nucleus)): Mean +/− SD, *N*=3 for YDFR.SB3, *N*=2 for WP.

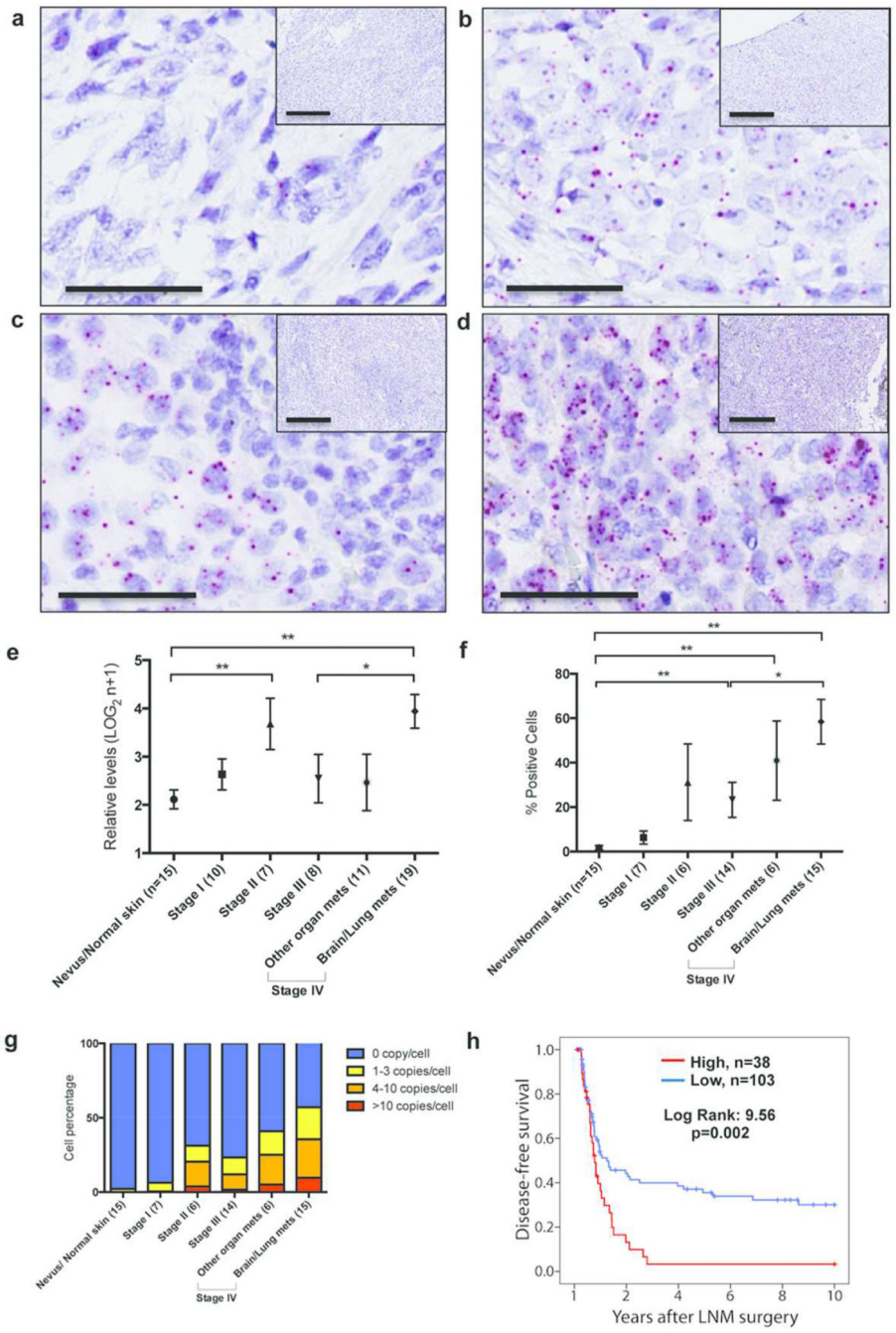

Figure 4.

CASC15 expression in melanoma specimens. (**a–d**) Representative *CASC15* RNA-ISH staining of archived melanoma specimens. (a) Primary melanoma with ≤1 copy/cell, (b) Primary melanoma with 1–3 copies/cell, (c) melanoma lymph node metastasis (LN mets) showing positive staining in melanoma cells and negative staining in lymphocytes, and (d) melanoma brain metastasis (Brain mets) showing strong staining (>4 copies/cell) in >30% of tumor cells. Scale bars = 50μm (panels) and 300μm (inserts). (**e**) RT-qPCR detection of *CASC15* expression levels (exon 8-containing isoforms) as a function of tumor stage. See

Table S1 for details. (LOG_2 (n+1) of $2^{-(ddCq)}$ relative values; T-test; *, $P<0.05$; **, $P<0.01$; Mean +/− SEM). (**f**) RNA-ISH detection of *CASC15* expression levels (exons 5–12) as a function of tumor stage. (% positive cells; Mann-Whitney test; *, $P<0.05$; **, $P<0.01$, Mean +/− SEM). (**g**) Same as in (**f**), organized according to the number of copies per cell. (average % of cells per category for each sample group). (**h**) Kaplan-Meier curves representing the relationship between *CASC15* expression in stage III melanoma LN mets and 10-year DFS.

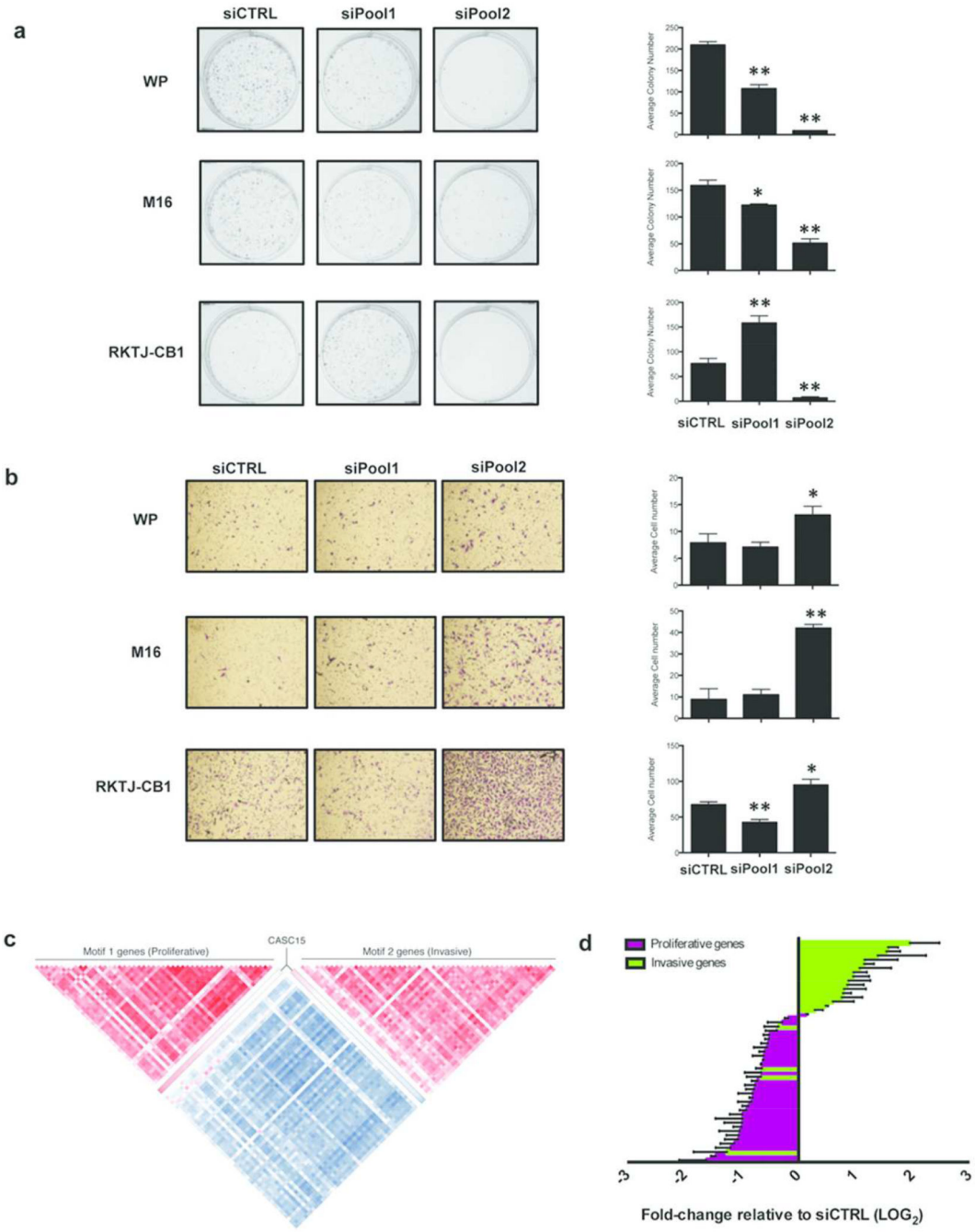

Figure 5.

CASC15 is involved in melanoma cell transition between proliferative and invasive states. (**a**) Clonogenic assays for WP, M16, and RKTJ-CB1 cell lines. Histograms depict the average colony number per condition for the respective cell line. (T-Test, **, $P<0.01$; *, $P<0.05$, Mean +/− SEM). Representative of 3 independent experiments. (**b**) Invasion assays for WP, M16, and RKTJ-CB1 cell lines. Histograms depict the average number of cells that crossed the invasion chamber per condition for the respective cell line. (T-Test, **, $P<0.01$; *, $P<0.05$, Mean +/− SEM). Representative of 3 independent experiments. (**c**) Correlation

(Spearman rho) between *CASC15* expression and proliferative/invasive gene signatures (Hoek *et al.*, 2006) in 47 melanoma cell lines. Red gradient: positive correlation. Blue gradient: negative correlation. Note the unequivocal inverse correlation between proliferative and invasive signature genes. (**d**) Effect of siPool2-mediated *CASC15* knockdown on the levels of 31 proliferative and 21 invasive signature genes (Table S8). Bars: SEM. Values below zero indicate down-regulation, and values above 0 indicate up-regulation relative to siCTRL (LOG_2 value of fold-change).